

Enhanced magnetocaloric effect in frustrated magnetic molecules with icosahedral symmetry

Jürgen Schnack*

Fakultät für Physik, Universität Bielefeld, Postfach 100131, D-33501 Bielefeld, Germany

Reimar Schmidt[†] and Johannes Richter[‡]

Institut für Theoretische Physik, Universität Magdeburg, P.O. Box 4120, D-39016 Magdeburg, Germany

(Received 19 March 2007; revised manuscript received 30 May 2007; published 7 August 2007)

We investigate the magnetocaloric properties of certain antiferromagnetic spin systems that have already been or very likely can be synthesized as magnetic molecules. It turns out that the special geometric frustration which is present in antiferromagnets that consist of corner-sharing triangles leads to an enhanced magnetocaloric effect with high cooling rates in the vicinity of the saturation field. These findings are compared with the behavior of a simple unfrustrated spin ring as well as with the properties of the icosahedron. To our surprise, also for the icosahedron large cooling rates can be achieved but due to a different kind of geometric frustration.

DOI: [10.1103/PhysRevB.76.054413](https://doi.org/10.1103/PhysRevB.76.054413)

PACS number(s): 75.50.Xx, 75.10.Jm, 75.40.Cx

I. INTRODUCTION

Antiferromagnetic finite-size spin systems with icosahedral symmetry constitute very interesting frustrated materials with rather unusual magnetic properties. Among such properties are jumps to the saturation magnetization in the cuboctahedron and the icosidodecahedron^{1,2} as well as metamagnetic phase transitions at zero temperature, for instance, in the icosahedron and dodecahedron.^{3–6} Some of these properties, for instance, the large magnetization jump to saturation, are as well present in the Kagome or other lattice antiferromagnets.⁷ The finite-size systems, nevertheless, have the advantage that due to their smallness many properties can be investigated (numerically) exactly with possible benefits for our knowledge about infinitely extended frustrated spin systems. In this paper, we investigate the magnetocaloric properties of certain spin clusters with icosahedral symmetry that turn out to be interesting as well.

Magnetocalorics has a long tradition especially in connection with cooling by adiabatic demagnetization. The first successful attempts to reach the sub-Kelvin region date back more than 70 years.⁸ It is equally well possible to extend such an adiabatic process to a full Carnot cycle and thus use the magnetization work for magnetic refrigeration.⁹ In the past, paramagnetic salts have been the working medium in both cases which limits the cooling rate to be not more than 2 K/T. Nowadays, gadolinium compounds such as Gd₅Ga₅O₁₂ or Gd₅Si₂Ge₂ are known to be very efficient refrigerant materials.^{10,11}

A unified explanation of a magnetocaloric effect that is enhanced compared to a paramagnet is provided by the observation that the cooling rate assumes extreme values close to configurations with a large excess entropy. This can happen at certain phase transitions such as the first order [ferromagnetic(I) ↔ ferromagnetic(II)] phase transition observed in Gd₅Si₂Ge₂ compounds,¹⁰ at magnetic field driven transitions across a quantum critical point,^{12,13} or at special values of the magnetic field where many ground-state Zeeman levels are degenerate.^{13–15}

In this paper, we demonstrate that an enhanced magnetocaloric effect should be observable in certain highly frus-

trated magnetic molecules of icosahedral symmetry. We discuss the cuboctahedron¹⁶ and the icosidodecahedron¹⁷ which are already synthesized Archimedean solids as well as the icosahedron which in its full symmetry could not yet be achieved chemically.^{16,18,19} For the structures of these bodies, we refer to the Appendix.

Some of the aspects of our investigation have been previously discussed in connection with the classical¹¹ as well as in the quantum version¹⁵ of the Kagome lattice antiferromagnet and some one-dimensional antiferromagnets.^{13,20} We also like to mention that magnetocaloric studies have been carried out in the field of molecular magnetism recently, but were mainly focused on low-field behavior.^{21–28}

This paper is organized as follows. In Sec. II, we discuss the basics of magnetocalorimetry, whereas in Sec. III, we present the magnetocaloric properties of icosahedral bodies and compare them with those of a nonfrustrated spin ring of the same size. This paper closes with a summary.

II. BASIC THERMODYNAMICS

A. Heisenberg model

The spin systems discussed in this paper are modeled by an isotropic Heisenberg Hamiltonian augmented with a Zeeman term, i.e.,

$$\underline{H} = - \sum_{u,v} J_{uv} \vec{s}(u) \cdot \vec{s}(v) + g \mu_B B \underline{S}_z. \quad (1)$$

$\vec{s}(u)$ are the individual spin operators at sites u , $\underline{S} = \sum_u \vec{s}(u)$ is the total spin operator, and \underline{S}_z its z component along the homogeneous magnetic field. J_{uv} are the matrix elements of the symmetric coupling matrix. A negative value of J_{uv} corresponds to antiferromagnetic coupling. For the symmetric polytopes discussed in the following, an antiferromagnetic nearest-neighbor exchange of constant size J is assumed.

Since the Hamiltonian commutes with \underline{S}_z , we can find a common eigenbasis $\{| \nu \rangle\}$ of both operators and denote the eigenvalues of \underline{H} by E_ν and of \underline{S}_z by M_ν , respectively. Due to the Zeeman term in Eq. (1), the energy eigenvalues $E_\nu = E_\nu(B)$ depend on the external magnetic field B . The field at

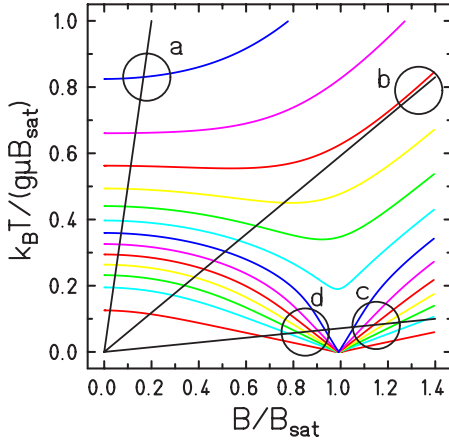


FIG. 1. (Color online) The curves show isentropes of the antiferromagnetically coupled dimer of two spins with $s=1/2$. The straight lines represent isentropes of a paramagnet. Compared to a paramagnet, the cooling rate of the antiferromagnetic dimer can be smaller (a), about the same (b), much bigger (c), or even negative (d).

which at $T=0$ the magnetization reaches its maximal value of $\mathcal{M}_{\text{sat}}=Ns$ is called saturation field B_{sat} .

B. Magnetocaloric effect

The magnetocaloric effect consists in cooling or heating of a magnetic system in a varying magnetic field. Some basic thermodynamics yields the adiabatic (i.e., isentropic, $S=\text{const}$) temperature change as a function of temperature and applied magnetic field,

$$\left(\frac{\partial T}{\partial B}\right)_S = -\frac{T}{C(T,B)} \left(\frac{\partial S}{\partial B}\right)_T. \quad (2)$$

This rate is also called cooling rate. $C(T,B)$ is the temperature- and field-dependent heat capacity of the system. For a paramagnet, this rate is simply¹¹

$$\left(\frac{\partial T}{\partial B}\right)_S^{\text{para}} = \frac{T}{B}. \quad (3)$$

This situation changes completely for an interacting spin system. Depending on the interactions, the adiabatic cooling

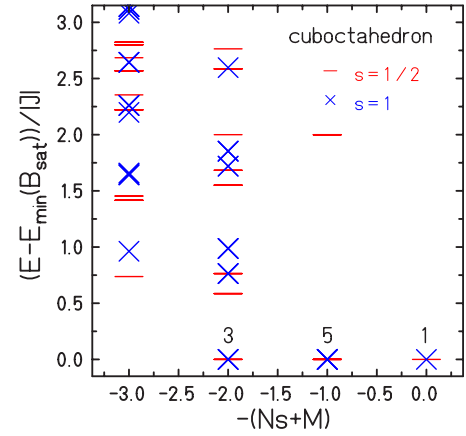


FIG. 2. (Color online) Low-lying energy levels $E_n(B)$ of the cuboctahedron with $s=1/2$ (dashes) and $s=1$ (\times symbols) at the saturation field $B=B_{\text{sat}}$ versus total magnetic quantum number M . The attached numbers give the multiplicities d_M of the lowest M levels. The energy scale (y axis) is organized in such a way that at $B=B_{\text{sat}}$ the lowest, i.e., ground-state levels are at zero and all other levels above.

rate $\frac{\partial T}{\partial B}$ can be smaller or bigger than the paramagnetic one and even change sign, i.e., one would observe heating during demagnetization and cooling during magnetization.^{13,28} For the purpose of clarity, this will be shortly illuminated with the help of an antiferromagnetically coupled dimer of two spins with $s=1/2$, where a singlet constitutes the ground state and a triplet the excited state. Following Eq. (2), one notices that in the vicinity of the magnetic field B_c , where the lowest triplet level crosses the singlet, the entropy changes drastically at low temperatures due to the fact that at the crossing field the ground state is degenerate whereas elsewhere it is not. This behavior is displayed in Fig. 1, where below and above the crossing field the cooling rate, i.e., the slope of the isentropes, assumes large values.

III. MAGNETOCALORIC EFFECT IN MAGNETIC MOLECULES

Regarding the use as a magnetic refrigerant material, magnetic molecules possess several advantageous properties. They can be synthesized in a great variety of structures and

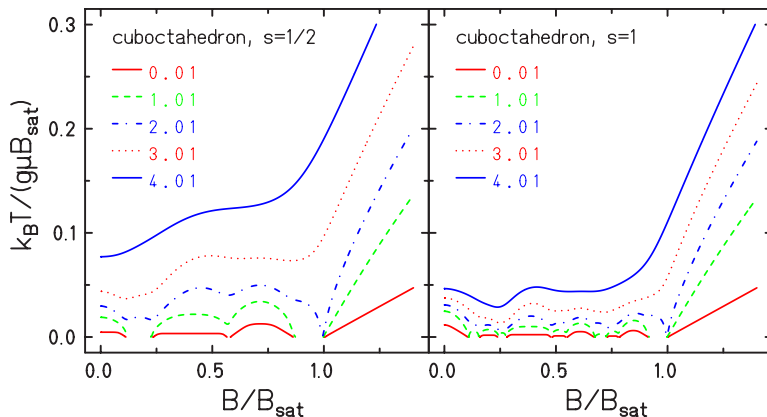


FIG. 3. (Color online) Isentropes of the cuboctahedron with $s=1/2$ and $s=1$. The entropies here and in the following are given in units of Boltzmann's constant k_B ; from the upper left to the lower right the values of S/k_B are 0.01, 1.01, 2.01, 3.01, and 4.01, respectively. $B_{\text{sat}} = (12s|J|)/(g\mu_B)$.

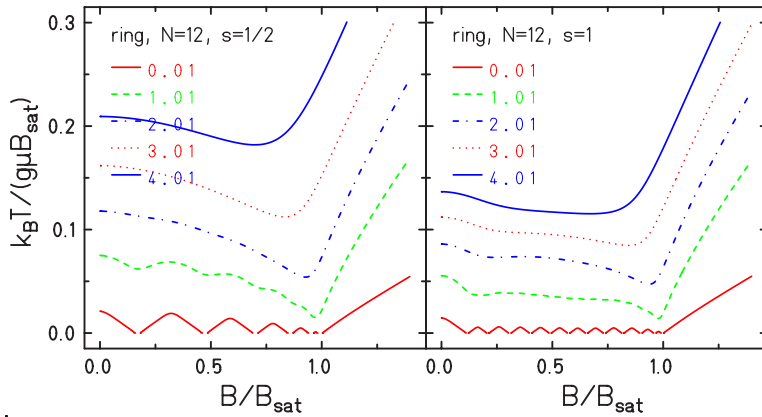


FIG. 4. (Color online) Isentropes of a bipartite, i.e., nonfrustrated spin ring with $N=12$ spins $s=1/2$ and $s=1$. $B_{\text{sat}}=(8s|J|)/(g\mu_B)$.

they can host various paramagnetic ions. Very often, they also do not interact magnetically with each other in a bulk sample due to large distances between the magnetic centers of different molecules that are provided by extended ligands, which means that the magnetic properties of a single molecule can be assigned to the macroscopic sample. If it would be possible to obtain structures which exhibit extraordinarily large ground-state degeneracies at certain magnetic fields, one could exploit these materials for very efficient magnetization cooling.

Every antiferromagnetically coupled spin system exhibits ground-state level crossings, such as the aforementioned spin dimer. The cooling rate at such a crossing can assume large values, but it turns out that it is possible to even increase the rate in a special class of highly frustrated magnetic molecules of icosahedral symmetry. This will be discussed for the cuboctahedron, which is chemically realized as a $\{\text{Cu}_{12}\text{La}_8\}$ molecule,¹⁶ and for the icosidodecahedron, which is chemically realized as a $\{\text{Mo}_{72}\text{Fe}_{30}\}$ molecule¹⁷ and a $\{\text{Mo}_{72}\text{V}_{30}\}$ molecule²⁹ as well as for the not yet synthesized icosahedron. The behavior of these frustrated spin systems is compared with the behavior of an antiferromagnetic, but not frustrated spin ring with $N=12$ sites. All results are obtained by means of numerical diagonalization.

The geometric structures of the discussed bodies are shown in the Appendix as well as, for instance, at Refs. 1, 2, and 30.

The cuboctahedron is one of the smallest antiferromagnetic spin systems that can host independent localized magnons.^{1,2,7} These localized states are intimately connected

with an enhanced degeneracy of energy levels and—in extended spin systems such as the Kagome lattice antiferromagnet—with the appearance of flatbands. In addition, the possibility to arrange several independent magnons on the (finite) spin lattice results in a linear dependence of the minimal energy $E_{\text{min}}(M)$ on the total magnetic quantum number M . Therefore, at the saturation field B_{sat} , a massive degeneracy of ground-state levels can be achieved.

Figure 2 shows that even in a system as small as the cuboctahedron the multiplicity of the ground state at the saturation field can reach a rather large value. As can be inferred from the numbers attached to the lowest levels in Fig. 2, the level with $M=-NS$ is nondegenerate, the lowest level with $M=-NS+1$ is fivefold degenerate, and the lowest level with $M=-NS+2$ is threefold degenerate. At B_{sat} , they are all energetically degenerate and constitute the ground-state manifold which altogether is then ninefold degenerate. This property is independent of spin quantum number, i.e., it holds for $s=1/2, 1, 3/2, \dots$ ^{1,2} Thus, the entropy assumes a nonzero value at zero temperature of $S_0=S(T=0, B=B_{\text{sat}})=k_B \ln(9)$. All isentropes with $S \leq S_0$ therefore arrive at the phase space point $(T=0, B=B_{\text{sat}})$.

Figure 3 displays various isentropes of the cuboctahedron both for $s=1/2$ [left-hand side (lhs)] as well as for $s=1$ [right-hand side (rhs)]. Both temperature and magnetic field are normalized to the saturation field here and in the following. One clearly sees that the low-entropy curves, $S \leq S_0$, approach the B axes, i.e., $T=0$, in a rather universal way independent of the magnitude of the spin s . Close to the saturation field, the slope of the isentropes, i.e., the cooling

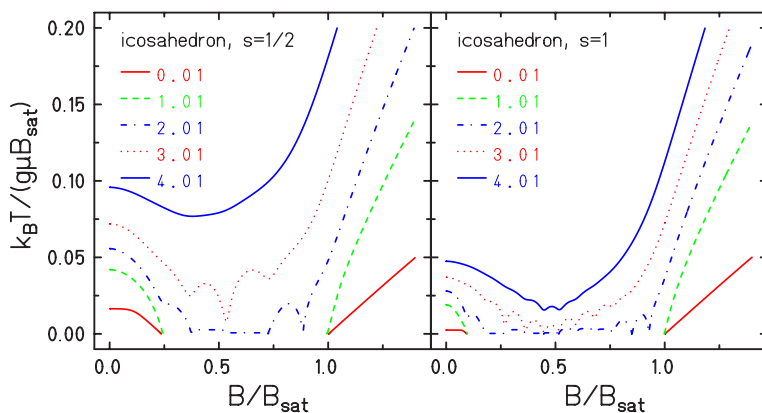


FIG. 5. (Color online) Isentropes of the icosahedron with $s=1/2$ and $s=1$. $B_{\text{sat}}=(14.472s|J|)/(g\mu_B)$.

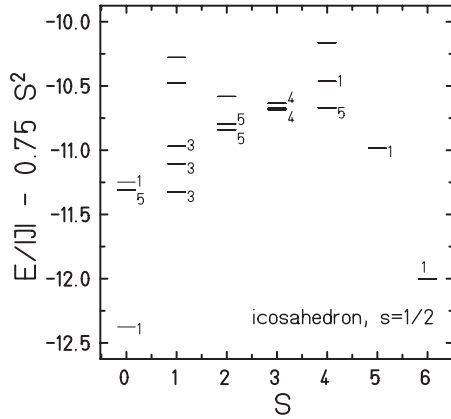


FIG. 6. Low-lying energy levels of the icosahedron with $s = 1/2$. The attached numbers give the multiplicity d_M of each M level. Note that the energies are rescaled in each sector of total spin S .

rate, can assume large values. Below the saturation field, the isentropes remain rather flat, i.e., the temperature does not increase again when going to $B=0$. This is of course an important property because otherwise the system would heat up again when switching off the field.

The nonfrustrated ring system, Fig. 4, does not possess the latter property nor does it exhibit large cooling rates at low temperatures close to the saturation field. The second property is easily understood because the massive degeneracy at the saturation field does not occur in an antiferromagnetic ring. Therefore, only isentropes with $S < k_B \ln(2)$ approach the field axis. The first property, however, is related to the overall structure of the low-lying levels. In finite bipartite systems, the levels are arranged in rotational bands^{31,32} which means that in each sector of total magnetic quantum number M the excited states are separated from the ground state in the respective sector by a nonvanishing gap. Thus, at lower magnetic fields, a certain entropy can only be realized by populating higher-lying levels, i.e., by acquiring a higher temperature.

The behavior of the icosahedron is intermediate. The antiferromagnetic icosahedron is also a geometrically frustrated spin system but differs from the cuboctahedron in some aspects. Each spin has five nearest neighbors (cuboctahedron—four), and the structure consists of edge-sharing triangles in-

stead of corner-sharing triangles as for the cuboctahedron. Therefore, the icosahedron does not possess independent one-magnon states and consequently a similar degeneracy at the saturation field cannot be expected, see Fig. 5.

Nevertheless, it turns out that the special frustration of the icosahedron leads to different (quasi) degeneracies in several Hilbert subspaces with total spin S . This can be seen in Fig. 6 where the low-lying levels of the icosahedron with $s = 1/2$ are displayed. Note that for better visibility the energies are rescaled in each sector of total spin S . The numbers display the multiplicities d_M of the M levels. These are the relevant degeneracies in an applied field. The total degeneracy at $B=0$ is $d = d_M(2S+1)$. Thus, we find also for the icosahedron that at certain magnetic field values, not necessarily at the saturation field, highly degenerate levels will cross and give rise to notable ($T=0$) entropy. This can, for instance, be observed for the isentrope with $S=2.01k_B$, which is displayed by the dashed-dotted line in Fig. 5. It approaches the field axis very closely at about $0.9B_{\text{sat}}$.

The unusually large degeneracy in many sectors of total spin is also the reason for the interesting property that the isentropes remain at rather small temperatures for decreasing magnetic fields. This is in strong contrast to spin rings and reflects the fact that populating the degenerate levels produces sufficient entropy without increasing the temperature. The upturn at small fields close to $B=0$ is mainly due to the nondegenerate ground state in the sector with $S=0$ which is separated by large gaps from excited states.

The two panels of Fig. 7 summarize the above discussion for the three systems with $N=12$ by comparing the isentropes with $S=2k_B$. One sees that at low temperatures close to the saturation field, the cuboctahedron indeed achieves the largest cooling rate. In the extreme quantum case, i.e., for $s = 1/2$, it also outperforms the two other systems when looking at the achievable temperatures for $B \rightarrow 0$. Nevertheless, for the icosahedron, similarly large cooling rates can be achieved due to a different kind of geometric frustration. For larger spin quantum numbers, i.e., for becoming more classical, the differences between the cuboctahedron and the icosahedron tend to disappear. The unfrustrated ring systems always show poorer cooling.

Finally, we like to discuss the behavior of the antiferromagnetic icosidodecahedron which also possesses icosahedral symmetry. This Archimedean solid is closely related to the cuboctahedron. It also consists of corner-sharing tri-

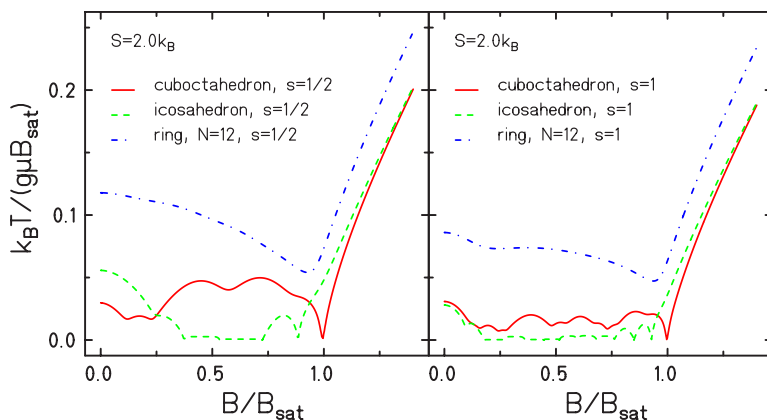


FIG. 7. (Color online) Isentropes with $S = 2k_B$ of the cuboctahedron, the icosahedron, and the ring with $N=12$ with spins $s=1/2$ (lhs) and $s=1$ (rhs).

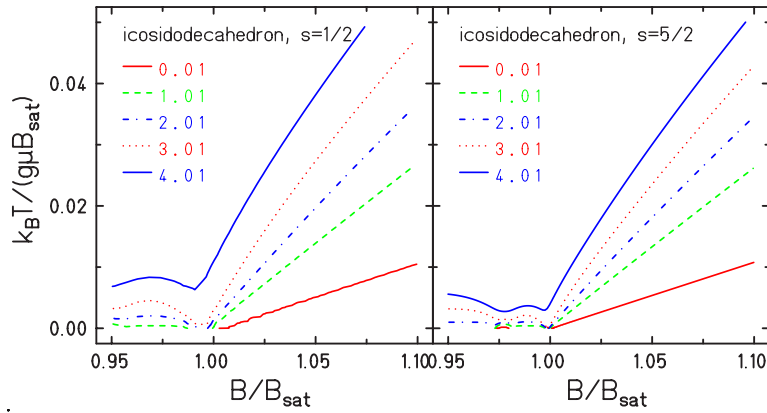


FIG. 8. (Color online) Isentropes of the icosidodecahedron with $s=1/2$ and $s=5/2$. $B_{\text{sat}} = (12s|J|)/(g\mu_B)$.

angles, and each spin has four nearest neighbors.^{2,30} But compared to the cuboctahedron, it has a much bigger ground-state degeneracy of 38 at the saturation field, again independent of spin quantum number. Figure 8 shows some isentropes of the icosidodecahedron for the two experimentally relevant cases of $s=1/2$ and $s=5/2$. Due to the much larger Hilbert space, these isentropes can be evaluated exactly only close to the saturation field since there are only some small subspaces that contribute. The magnetothermal behavior is very similar to the cuboctahedron with the noticeable difference that now isentropes with entropies up to $S_0 = S(T=0, B=B_{\text{sat}}) = k_B \ln(38) \approx 3.63k_B$ head toward $T=0$ at the saturation field.

IV. SUMMARY

In summary, we can say that the investigated frustrated antiferromagnetic bodies show an enhanced cooling rate in comparison with nonfrustrated (bipartite) spin rings. This rate is especially large for those systems that show a large degeneracy of levels, either at the saturation field (cuboctahedron and icosidodecahedron) or elsewhere (icosahedron).

We like to mention that similar effects can be observed in interacting electron systems described by the Hubbard model. This is related to the appearance of flatbands in these systems.^{33–36}

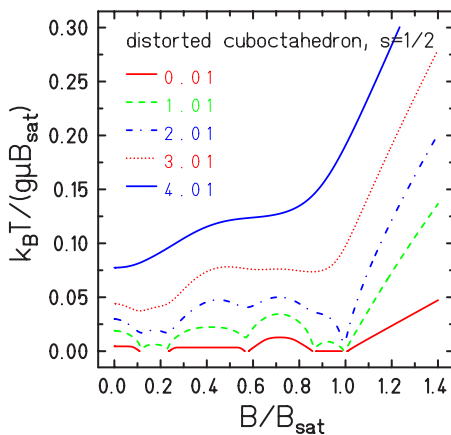


FIG. 9. (Color online) Isentropes of a distorted cuboctahedron with $s=1/2$. Each coupling J_{ij} between spins at sites i and j was modified by a random distortion of maximally $\pm 5\%$.

A few words seem to be in order regarding the question of how realistic the outlined scenario is. In realistic systems, the perfect degeneracy of levels at the saturation field will certainly be lifted, thus keeping the entropy $S(T=0, B=B_{\text{sat}})$ at a small value. Nevertheless, the low-energy density of states will remain large in the vicinity of the saturation field, since the originally degenerate levels move not too far, thus the magnetothermal properties will be left qualitatively unchanged.¹⁴

To make this point clearer, we have evaluated the isentropes of several distorted cuboctahedra where each original coupling J_{ij} between spins at sites i and j was modified by a random distortion of maximally $\pm 5\%$. All samples lead to very similar isentropes; Fig. 9 shows the resulting isentropes of one typical sample. As said before, a distortion of this order of course lifts the perfect ninefold degeneracy of the cuboctahedron at the saturation field. This can be seen by looking at the dashed-dotted curve for $S/k_B=2.01$ which now no longer touches the x axis. Nevertheless, the slope of the isentropes both around the saturation field and elsewhere is practically unchanged due to the fact that the density of states is rather robust against small random modifications of the exchange integrals J_{ij} .

The main source of any enhanced magnetocaloric effect is of course a large isothermal entropy change as a function of magnetic field, which—as shown—is the case if many energy levels coincide at a certain field. This could also be the

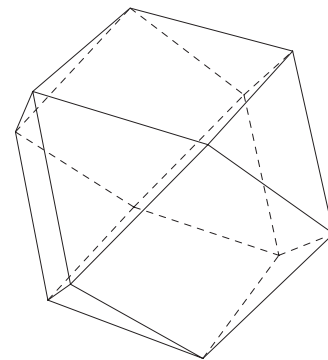


FIG. 10. Three-dimensional projection of the cuboctahedron (Ref. 30). The vertices are spin sites and the lines denote the anti-ferromagnetic coupling with exchange parameter J . Each spin has four nearest neighbors.

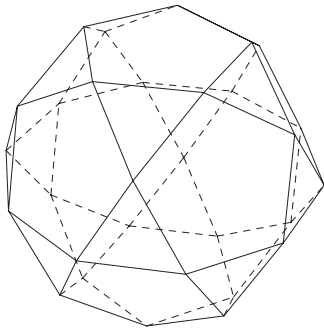


FIG. 11. Three-dimensional projection of the icosidodecahedron (Ref. 30). The vertices are spin sites and the lines denote the antiferromagnetic coupling with exchange parameter J . Each spin has four nearest neighbors.

case for so-called molecular magnets, i.e., molecules with a large ground-state spin. Such a scenario is discussed in Ref. 27. The performance of the achievable cooling depends on the achievable degeneracy of levels. Thus, a molecular magnet with high ground-state spin could be as well a good cooling material if these levels are not split by anisotropy.

ACKNOWLEDGMENT

J. R. and R. S. greatly acknowledge the use of SPINPACK, a software provided by Jörg Schulenburg.

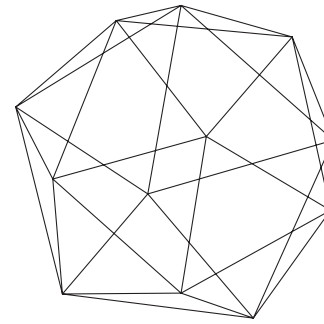


FIG. 12. Three-dimensional projection of the icosahedron (Ref. 30). The vertices are spin sites and the lines denote the antiferromagnetic coupling with exchange parameter J . Each spin has five nearest neighbors.

APPENDIX: STRUCTURES OF THE CUBOCTAHEDRON, THE ICOSIDODECAHEDRON, AND THE ICOSAHEDRON

Figures 10–12 show the geometric structures of the cuboctahedron, the icosidodecahedron, and the icosahedron, respectively. All of these structures lead to geometric frustration in the case of antiferromagnetic interaction due to the presence of triangles. The first two polytopes consist of corner-sharing triangles, whereas the icosahedron consists of edge-sharing triangles. The latter structure leads to a different type of frustration which is less investigated than that of corner-sharing triangles.

*jschnack@uni-bielefeld.de

†reimar.schmidt@phyisk.uni-magdeburg.de

‡Johannes.Richter@physik.uni-magdeburg.de

¹R. Schmidt, J. Schnack, and J. Richter, *J. Magn. Magn. Mater.* **295**, 164 (2005).

²J. Schnack, H.-J. Schmidt, J. Richter, and J. Schulenburg, *Eur. Phys. J. B* **24**, 475 (2001).

³D. Coffey and S. A. Trugman, *Phys. Rev. Lett.* **69**, 176 (1992).

⁴C. Schröder, H.-J. Schmidt, J. Schnack, and M. Luban, *Phys. Rev. Lett.* **94**, 207203 (2005).

⁵N. P. Konstantinidis, *Phys. Rev. B* **72**, 064453 (2005).

⁶N. P. Konstantinidis, arXiv:cond-mat/0610218 (unpublished).

⁷J. Schulenburg, A. Honecker, J. Schnack, J. Richter, and H.-J. Schmidt, *Phys. Rev. Lett.* **88**, 167207 (2002).

⁸W. F. Giaque and D. MacDougall, *Phys. Rev.* **43**, 768 (1933).

⁹V. K. Pecharsky and K. A. Gschneidner, *J. Magn. Magn. Mater.* **200**, 44 (1999).

¹⁰V. K. Pecharsky and K. A. Gschneidner, *Phys. Rev. Lett.* **78**, 4494 (1997).

¹¹M. E. Zhitomirsky, *Phys. Rev. B* **67**, 104421 (2003).

¹²L. J. Zhu, M. Garst, A. Rosch, and Q. M. Si, *Phys. Rev. Lett.* **91**, 066404 (2003).

¹³M. E. Zhitomirsky and A. Honecker, *J. Stat. Mech.: Theory Exp.* P07012 (2004).

¹⁴O. Derzhko and J. Richter, *Phys. Rev. B* **70**, 104415 (2004).

¹⁵M. E. Zhitomirsky and H. Tsunetsugu, *Prog. Theor. Phys. Suppl.* **160**, 361 (2005).

¹⁶A. J. Blake, R. O. Gould, C. M. Grant, P. E. Y. Milne, S. Parsons, and R. E. P. Winpenny, *J. Chem. Soc. Dalton Trans.* **1997**, 485.

¹⁷A. Müller, S. Sarkar, S. Q. N. Shah, H. Bögge, M. Schmidtman, S. Sarkar, P. Kögerler, B. Hauptfleisch, A. Trautwein, and V. Schünemann, *Angew. Chem., Int. Ed.* **38**, 3238 (1999).

¹⁸E. K. Brechin, A. Graham, S. G. Harris, S. Parsons, and R. E. P. Winpenny, *J. Chem. Soc. Dalton Trans.* **1997**, 3405.

¹⁹E. I. Tolis *et al.*, *Chem.-Eur. J.* **12**, 8961 (2006).

²⁰O. Derzhko and J. Richter, *Eur. Phys. J. B* **52**, 23 (2006).

²¹R. D. McMichael, R. D. Shull, L. J. Swartzendruber, L. H. Bennett, and R. E. Watson, *J. Magn. Magn. Mater.* **111**, 29 (1992).

²²L. H. Bennett, R. D. McMichael, H. C. Tang, and R. E. Watson, *J. Appl. Phys.* **75**, 5493 (1994).

²³F. Torres, J. M. Hernandez, X. Bohigas, and J. Tejada, *Appl. Phys. Lett.* **77**, 3248 (2000).

²⁴X. X. Zhang, H. L. Wei, Z. Q. Zhang, and L. Zhang, *Phys. Rev. Lett.* **87**, 157203 (2001).

²⁵F. Torres, X. Bohigas, J. M. Hernandez, and J. Tejada, *J. Phys.: Condens. Matter* **15**, L119 (2003).

²⁶M. Affronte, A. Ghirri, S. Carretta, G. Amoretti, S. Piligkos, G. A. Timco, and R. E. P. Winpenny, *Appl. Phys. Lett.* **84**, 3468 (2004).

²⁷M. Evangelisti, A. Candini, A. Ghirri, M. Affronte, E. K. Brechin, and E. J. McInnes, *Appl. Phys. Lett.* **87**, 072504 (2005).

²⁸O. Waldmann, R. Koch, S. Schromm, P. Müller, I. Bernt, and R. W. Saalfrank, *Phys. Rev. Lett.* **89**, 246401 (2002).

²⁹A. Müller, A. M. Todea, J. van Slageren, M. Dressel, H. Bögge,

- M. Schmidtman, M. Luban, L. Engelhardt, and M. Rusu, *Angew. Chem., Int. Ed.* **44**, 3857 (2005).
- ³⁰E. Weisstein, Mathworld, <http://mathworld.wolfram.com>
- ³¹J. Schnack and M. Luban, *Phys. Rev. B* **63**, 014418 (2001).
- ³²O. Waldmann, *Phys. Rev. B* **65**, 024424 (2001).
- ³³H. Tasaki, *Phys. Rev. Lett.* **69**, 1608 (1992).
- ³⁴A. Mielke, *J. Phys. A* **25**, 4335 (1992).
- ³⁵A. Honecker and J. Richter, *Condens. Matter Phys.* **8**, 813 (2005).
- ³⁶O. Derzhko, A. Honecker, and J. Richter, arXiv:cond-mat/0703295 (unpublished).